Proc. Natl. Acad. Sci. USA
Vol. 90, pp. 9552–9556, October 1993
Cell Biology

Mechanism of mitotic block and inhibition of cell proliferation by taxol at low concentrations

(HeLa cells/microtubule dynamics/vinblastine)

MARY ANN JORDAN*, ROBERT J. TOSO, DOUG THROWER, AND LESLIE WILSON

Department of Biological Sciences, University of California, Santa Barbara, CA 93106-9610

Communicated by John Carbon, July 14, 1993 (received for review June 8, 1993)

ABSTRACT **Taxol inhibited HeLa cell proliferation by inducing a sustained mitotic block at the metaphase/anaphase boundary. Half-maximal inhibition of cell proliferation occurred at 8 nM taxol, and mitosis was half-maximally blocked at 8 nM taxol. Inhibition of mitosis was associated with formation of an incomplete metaphase plate of chromosomes and an altered arrangement of spindle microtubules that strongly resembled the abnormal organization that occurs with low concentrations of vinblastine and other antimitotic compounds. No increase in microtubule polymer mass occurred below 10 nM taxol. The mass of microtubules increased half-maximally at 80 nM taxol and attained maximal levels (5 times normal) at 330 nM taxol. At submicromolar concentrations, taxol suppressed growing and shortening at the ends of microtubules reassembled *in vitro* from bovine brain tubulin in a manner that resembled suppression by vinblastine. Taxol was concentrated in HeLa cells several hundredfold to levels that were similar to those which suppressed dynamic instability *in vitro*. The results indicate that taxol shares a common antiproliferative mechanism with vinblastine. At its lowest effective concentrations, taxol appears to block mitosis by kinetically stabilizing spindle microtubules and not by changing the mass of polymerized microtubules.**

The antimitotic antitumor drug taxol has undergone extensive clinical development as a result of its efficacy in the treatment of refractory ovarian cancer and its potential value for the treatment of breast, lung, and other cancers (1). The mechanism of action of taxol has been considered to be unique. The target for taxol appears to be microtubules, and in contrast to vinblastine, colchicine, and other antimitotic compounds that can inhibit microtubule polymerization both *in vitro* and in cells, taxol can enhance microtubule polymerization (2, 3). Taxol can block mitosis, induce extensive formation of microtubule bundles in cells, and induce multinucleation of cells during interphase (4–6). Enhanced microtubule polymerization has been suggested to be responsible for the antitumor activity of the drug.

However, in recent studies, we found (7–9) that at their lowest effective concentrations, vinblastine and vincristine inhibit mitosis and cell proliferation in HeLa cells without decreasing the mass of microtubules and with only subtle changes in the organization of the mitotic spindles. We also found that low concentrations of vinblastine inhibit dynamic instability and treadmilling of reassembled bovine brain microtubules *in vitro* without appreciably affecting the microtubule polymer mass (10, 11). Dynamic instability consists of transitions between phases of growing and phases of shortening at microtubule ends. Treadmilling is the net addition of tubulin at one microtubule end and the balanced net loss of tubulin at the opposite microtubule end. Both kinds of dynamics have been shown to occur in mitotic spindle microtubules, which are characterized by very rapid dynamic behaviors (for review, see ref. 12). Mitotic block at low concentrations of vinblastine is thought to occur by suppression of tubulin exchange at ends of mitotic spindle microtubules (7, 8, 11).

In the present study, we found that low concentrations of taxol inhibited mitosis in HeLa cells and suppressed dynamic instability at the ends of bovine brain microtubules *in vitro* in the absence of enhanced microtubule polymerization. In addition, inhibition of mitosis was associated with an altered organization of mitotic spindles that was strikingly similar to that induced by the vinca alkaloids and several other antimitotic drugs, suggesting that mitotic block and inhibition of proliferation by all of these drugs, including taxol, at their lowest effective concentrations, involves kinetic stabilization of mitotic spindle microtubule dynamics rather than alterations in microtubule polymer mass.

MATERIALS AND METHODS

HeLa S3 cells (American Type Culture Collection) were grown in monolayers at 37°C without antibiotics in 5% CO_2/95% air (7). Cell proliferation was determined by counting cells by hemocytometer at the time of taxol addition and 20 h later. Mitotic index, cell morphology, and spindle interpolar distances were determined by immunofluorescence microscopy (8). Levels of polymerized tubulin in cells were determined by measuring the tubulin content of isolated stabilized cytoskeletons by an ELISA (two to six determinations per taxol concentration) (13).

For analysis of the effects of taxol on dynamic instability, microtubules were assembled to steady state by adding bovine brain tubulin (depleted of microtubule-associated proteins, >99% tubulin, 1.5 mg/ml in 100 mM Mes/1 mM EGTA/1 mM $MgSO_4$/1 mM GTP, pH 6.7, 30°C) in the continuous presence of taxol onto the ends of *Strongylocentrotus purpuratus* sperm flagella axonemal seeds (11). Under the conditions used, control microtubules grow mainly at the plus ends of the seeds. Microtubules at the minus ends were few in number and very short. In the presence of taxol at the concentrations used, the microtubules at the two ends of the seeds were indistinguishable in length, number, and dynamics, and thus the measurements represent a mixture of microtubules at both ends of the seeds. Measurements of microtubule lengths were made at 15-s intervals from images captured using a Hamamatsu C2400 (Newvicon) video camera with video-enhanced differential interference contrast microscopy on a Zeiss IM35 microscope with a temperature-controlled stage (11). At least 100 measurements of an average of seven microtubules from a minimum of two experiments were used for each experimental condition.

The publication costs of this article were defrayed in part by page charge payment. This article must therefore be hereby marked "*advertisement*" in accordance with 18 U.S.C. §1734 solely to indicate this fact.

*To whom reprint requests should be addressed.

Taxol uptake into HeLa cells was determined after incubating cells for 20 h with [^{3}H]taxol (3–1000 nM; specific activity, 4–3600 Ci/mol; 1 Ci = 37 GBq) (7). Taxol and [^{3}H]taxol were gifts from the National Cancer Institute ([3′-^{3}H]taxol, NSC 125973) or were purchased (Moravek Biochemicals, La Brea, CA). [^{14}C]Hydroxymethylinulin (5.4 μM; specific activity, 10 Ci/mol; New England Nuclear) was added to cell suspensions before collection to determine extracellular volume.

RESULTS

Relationship of Inhibition of Cell Proliferation, Mitotic Block, and Enhancement of Microtubule Polymer Levels by Taxol. HeLa cells were incubated for the duration of one cell cycle with taxol over a broad range of concentrations. After 20 h, cytoskeletons were isolated to determine the mass of tubulin in the form of microtubules. In parallel experiments, inhibition of proliferation and mitotic indices were determined. Taxol inhibited cell proliferation half-maximally at a concentration of 8 nM, and inhibition was complete at concentrations >33 nM (Fig. 1*A*). Taxol induced the accumulation of cells in mitotic metaphase half-maximally at a concentration of ≈8 nM, and maximal mitotic accumulation (80–95%) occurred at taxol concentrations of 33 nM and above. Thus mitotic accumulation occurred in parallel with inhibition of proliferation. No increase in microtubule polymer mass occurred at <10 nM taxol. The mass of microtubules then increased as the taxol concentration was raised, attaining a half-maximal increase at a concentration of 80 nM and a maximal increase of 500% of the normal level at 330 nM taxol.

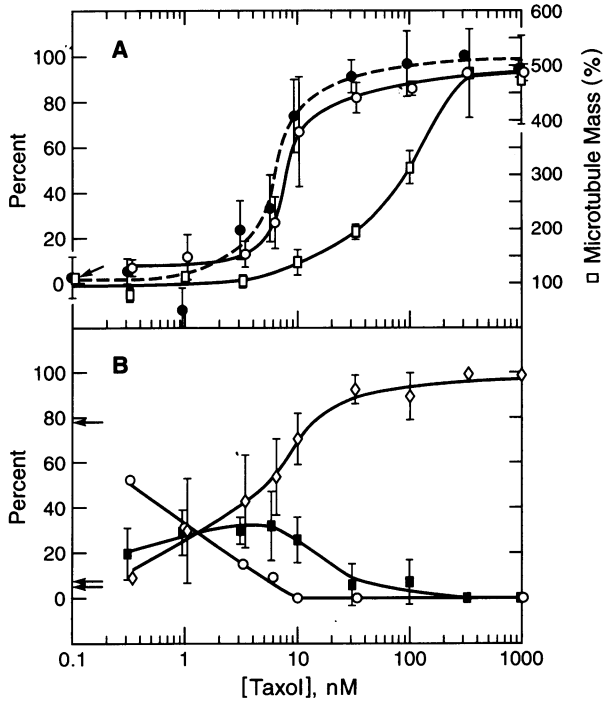

FIG. 1. (*A*) Taxol concentration dependence for metaphase arrest (open circles, left axis; arrow denotes control value), for inhibition of proliferation (solid circles, left axis), and for the increase in microtubule mass (open squares, right axis). (*B*) Taxol concentration dependence of spindle organization in HeLa cells after incubation with taxol for one cell cycle. (*A*) Accumulation of cells in metaphase was concomitant with inhibition of proliferation but was accompanied by little or no increase in the mass of microtubule polymer. (*B*) Percentages of metaphases that were normal (open circles), abnormal bipolar types I or II (solid squares), and ball-shaped type III (open diamonds). Arrows denote control values for normal metaphases (upper arrow), abnormal bipolar (middle arrow), and ball (lower arrow).

Cells accumulated in metaphase or in a metaphase-like configuration (see below), but no cells were in anaphase either after a 20-h incubation with 10 nM taxol (Table 1) or during long-term incubation (as long as 48 h) with 10 nM taxol (data not shown). Thus accumulation in mitosis represents a sustained block at the metaphase/anaphase boundary. Of the cells that were in interphase at low taxol concentrations (3–10 nM), a large percentage (31–38%) consisted of cells with two, three, or more nuclei (Table 1). These results suggest that the mitotic block induced by low taxol concentrations is not as sustained as at higher taxol concentrations; some cells can escape from mitotic block and become abnormal multinucleate cells.

Effects of Taxol on Spindle Organization. The arrangements of microtubules, chromosomes, and centrosomes of control cells and of cells incubated with taxol are shown in Fig. 2. Mitotic spindles of cells blocked in metaphase by low concentrations of taxol strongly resembled spindles of cells blocked by low concentrations of other antimitotic drugs including vinblastine, vincristine, nocodazole, colchicine, and podophyllotoxin (7, 8). Some spindles were blocked in a bipolar configuration that was normal (data not shown); chromosomes were all contained in a compact metaphase plate. Other spindles (20–32% with 0.33–10 nM taxol) were blocked in a nearly normal configuration; these spindles were bipolar with a compact metaphase plate of chromosomes but with some chromosomes located near the spindle poles (Fig. 2 *d–f*) (spindle types I and II, ref. 8). Astral microtubules in taxol-blocked spindles appeared more prominent than in control spindles, and the central spindle (the distance from pole to pole) was shorter than in control spindles. For example, the length of the central spindle was reduced from 7.4 ± 0.2 μm in control spindles to 4.0 ± 0.4 μm in bipolar spindles by 10 nM taxol (Table 1).

With increasing concentrations of taxol, spindle morphology became more abnormal; increasing numbers of chromosomes were located near the poles of bipolar spindles rather than in the metaphase plate (data not shown). Also as the taxol concentration was increased, many spindles had no bipolar organization but were ball-shaped aggregations of condensed chromosomes containing one or more asters of microtubules (Fig. 2 *g–i*). These resembled classical colchicine mitoses (C-mitoses of ref. 14) or type III aberrant spindles (8). The decrease in the proportions of bipolar (normal and aberrant types I and II) spindles and the increase in proportion of ball-shaped (type III) spindles with increasing taxol concentration are shown in Fig. 1*B*.

Table 1. Effects of taxol (20-h incubation) on metaphase/anaphase transition, multinucleation, and spindle pole separation

Taxol, nM	Cells in anaphase/ cells in metaphase, no./no.	Multinucleated interphase cells, %	Interpolar distance, μm
0	0.14 ± 0.03	2.7 ± 0.7	7.4 ± 0.2
0.3	0.09 ± 0.04	3.2 ± 1.2	6.6 ± 0.1
1	0.11 ± 0.05	11.6 ± 4.0	6.9 ± 0.1
3	0.04 ± 0.04	31.2 ± 17.9	6.1 ± 0.5
6	0.007 ± 0.004	32.6 ± 12.6	—
10	0	37.7 ± 11.5	4.0 ± 0.4
33	0	16.5 ± 4.5	2.8 ± 0.2
100	0	14.0 ± 6.8	—
1000	0	7.3 ± 2.3	—

Data are the mean ± SEM of three experiments for the ratio of cells in anaphase to metaphase and the percent multinucleated interphase cells (multinucleated cells have more than one nucleus). The interpolar distance is the distance between centrosomes at opposite spindle poles (mean ± SEM of ≥25 spindles).

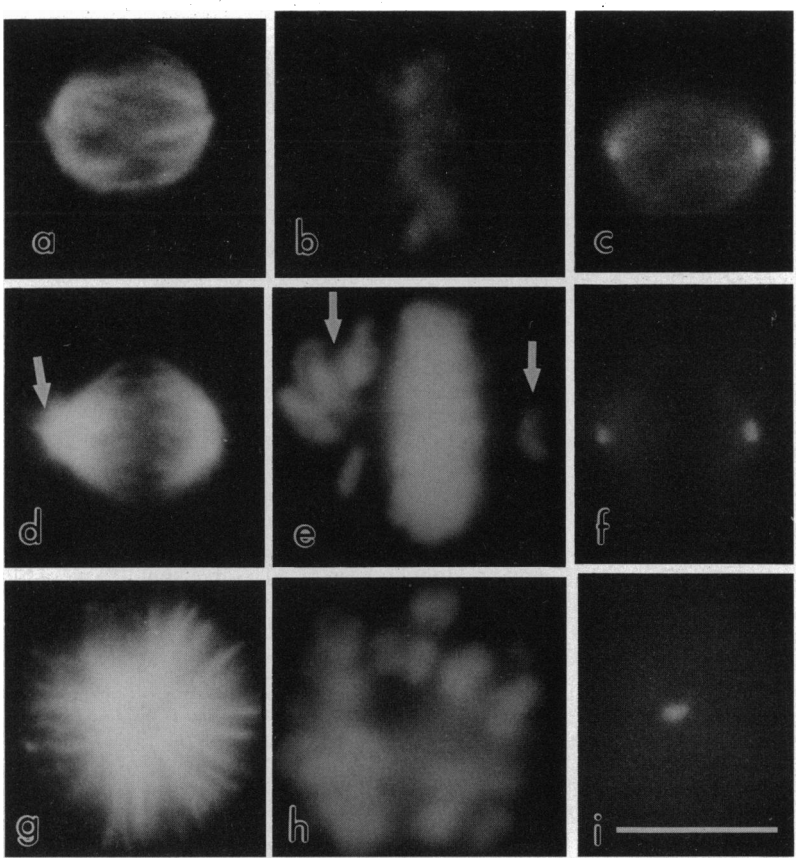

FIG. 2. Microtubules (*a*, *d*, and *g*), chromosomes (*b*, *e*, and *h*), and centrosomes (*c*, *f*, and *i*) of HeLa cell mitotic spindles after incubation for 18–20 h with taxol. (*a–c*) Control cell spindle with few astral microtubules and a well-defined compact metaphase plate of chromosomes. (*d–f*) At 6 nM taxol, an abnormal bipolar spindle (type I) with prominent astral microtubules (arrow in *d*) and chromosomes near the spindle poles (arrows in *e*). (*g–i*) At 1 μM taxol, a ball-shaped chromosomal mass with a monopolar microtubule and centrosome arrangement (type III). (Bar = 10 μm.)

The morphological changes in spindle structure induced by taxol were nearly identical to those that occurred with other antimitotic drugs (7, 8). However, there were some minor differences. Some bipolar spindles blocked by low concentrations of taxol appeared to have reduced numbers of interpolar microtubules (data not shown), in contrast with the bipolar spindles induced by low concentrations of other antimitotic drugs that appeared to have normal numbers of interpolar microtubules. This observation with taxol is consistent with the finding that addition of 10–20 μM taxol to PtK1 cells in early anaphase caused the disappearance of most interzonal microtubules within 5 min (15). In addition, in the present work upon incubation with 10–100 nM taxol, some mitotic asters contained no centrosomes (data not shown). Similar results were obtained in PtK2 cells after incubation with micromolar concentrations of taxol (16, 17).

Induction of Microtubule Bundling. Microtubule bundles did not form in the taxol concentration range in which little or no increase in microtubule mass occurred (1–10 nM). However, with 10 nM taxol, microtubules often became oriented in parallel fashion. (Compare the meshwork of microtubules of a control cell in interphase in Fig. 3*a* with the array of parallel microtubules radiating out from the nucleus after incubation with 10 nM taxol in Fig. 3*b*.) Loosely packed bundles of microtubules were observed in a few cells incubated with 33 nM taxol (Fig. 3*c*), a concentration at which the microtubule polymer mass was double that of control cells. Massive bundles of microtubules formed at higher taxol concentrations (e.g., 1 μM, Fig. 3*d*).

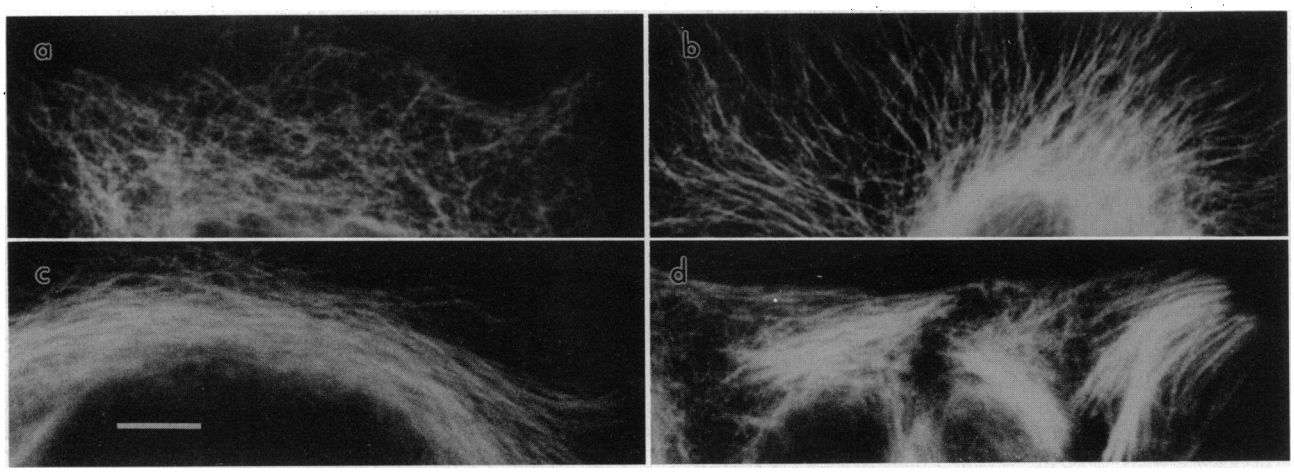

FIG. 3. Microtubules of HeLa cells in interphase incubated for 18–20 h with taxol. (*a*) Control irregular meshwork of microtubules. (*b*) At 10 nM taxol, a somewhat parallel alignment of microtubules but absence of microtubule bundles. (*c*) At 33 nM taxol, a loosely packed bundle of microtubules. (*d*) At 1 μM taxol, three compact bundles of microtubules. (Bar = 10 μm.)

Table 2. Suppression of microtubule dynamic instability by taxol

Taxol, μM	Growing rate, tubulin dimers per s	Shortening rate, tubulin dimers per s	% time in attenuation	Transition frequency from G or S to A	Dynamicity, tubulin dimers per s
0 (control)	106 ± 13	104 ± 16	19 ± 3	0.65	83 ± 8
0.1	59 ± 6	55 ± 4	45 ± 1	1.6	31 ± 4
0.5	48 ± 3	49 ± 5	53 ± 8	2.3	23 ± 2

Attenuation is a phase of no detectable length change at the microtubule ends. Transition frequency is the number of transitions divided by the total time the microtubules spent in the phases from which the transition occurred (11). G, growing; S, shortening; A, attenuation. Dynamicity is the total tubulin exchange in tubulin dimers per s (11). Control data are the same as in ref. 11.

Suppression of Dynamic Instability at Microtubule Ends *in Vitro*. Video microscopy was used to determine the effects of taxol on dynamic instability at ends of individual bovine brain microtubules. Taxol (0.1 and 0.5 μM) significantly inhibited the microtubule shortening rate and the microtubule growing rate and strongly inhibited the overall exchange of tubulin at microtubule ends (dynamicity, Table 2). Taxol increased the percentage of total time that the microtubules remained in an attenuated state, neither growing nor shortening detectably, from 19% in controls to >50% at 0.5 μM taxol. Taxol also increased the frequency of transition or switching from growing or shortening to attenuation. The suppression of dynamic instability by 0.1 and 0.5 μM taxol occurred without any detectable increase in the mass of polymerized tubulin (an increase in sedimentable microtubule polymer was detected under the conditions of the video microscopy only at taxol concentrations of ≥1 μM; W. B. Derry, L.W., and M.A.J., unpublished data).

Intracellular Taxol Concentration. Fifty percent mitotic block occurred at an added taxol concentration of 8 nM, a concentration that is far below that necessary to suppress microtubule dynamics *in vitro*. Thus, we measured the intracellular taxol concentration after incubation of cells with radiolabeled taxol at concentrations that induced mitotic block (Table 3). At all concentrations, taxol was concentrated several hundredfold intracellularly, to micromolar levels. For example, with 10 nM taxol, which induced 67 ± 24% mitotic block, 96% aberrant spindles, and multinucleation of 38% of the cells that were in interphase (Fig. 1*A* and Table 1), the drug was concentrated 480-fold to an intracellular level of 4.8 ± 0.7 μM. Therefore, while the subcellular location of all the taxol is not completely known (18), the overall intracellular taxol concentration was sufficient to suppress microtubule dynamics.

DISCUSSION

Very low concentrations of taxol are sufficient to inhibit proliferation of HeLa cells. Both half-maximal inhibition of proliferation and 50% blockage in mitotic metaphase occurred at 8 nM taxol. The degree of metaphase block by taxol paralleled the degree of inhibition of cell proliferation at all taxol concentrations. Inhibition was associated with formation of an incomplete metaphase plate of chromosomes and an arrangement of spindle microtubules that strongly resembled the abnormal organization that occurs with low concentrations of vinblastine and other antimitotic drugs (8). The most sensitive inhibitory effects of taxol on proliferation were not associated with an increase in microtubule polymer mass or with the formation of microtubule bundles, actions of taxol that occur at relatively high drug concentrations. No increase in microtubule polymer mass occurred below a taxol concentration of 10 nM (Fig. 1*A*), and 80 nM taxol was required to induce a half-maximal increase in the microtubule polymer mass. Thus these results indicate that the most sensitive action of taxol on HeLa cell proliferation involves blockage of cell cycle progression at the metaphase/anaphase transition in the presence of a normal mass of microtubule polymer.

Table 3. Intracellular taxol concentration in HeLa cells

Taxol in medium at time 0, μM	Taxol in cells at 20 h, μM	Fold uptake	Tubulin in polymer, μM
0.003	1.8 ± 0.3	600	6.3 ± 0.8
0.01	4.8 ± 0.7	480	8.4 ± 1.5
0.1	40.5 ± 8.0	405	19.1 ± 1.8
1.0	111.0 ± 13.8	111	28.8 ± 2.9

Amount of tubulin in polymer is from data of Fig. 1*A*, assuming total tubulin at 2 mg/ml and 31–36% in polymer in control cells (7).

Submicromolar concentrations of taxol significantly altered dynamic instability of microtubules *in vitro*. At plus ends, taxol inhibited both the rates of growing and shortening, strongly increased the percentage of time the microtubules remained in an attenuated state (neither growing nor shortening detectably), and increased the frequency of transition into periods of no detectable length change. Overall, taxol (0.5 μM) inhibited dynamicity by 70% (Table 2).

Interestingly, the inhibitory effects of taxol on dynamic instability qualitatively resemble those of vinblastine at the kinetically rapid microtubule plus ends (11). Like taxol, vinblastine strongly suppresses the rates of growing and shortening, increases the percentage of time that the microtubules spend in an attenuated state, increases the frequency of transition from growing or shortening to attenuation, and strongly suppresses dynamicity. Thus, while vinblastine and taxol interact with microtubules by different molecular mechanisms (3, 19–21), both drugs kinetically stabilize microtubule ends in a remarkably similar fashion. Thus, the data indicate that at low drug concentrations, taxol may share a common antiproliferative mechanism with vinblastine in HeLa cells, namely, inhibition of mitosis by suppressing the dynamics of mitotic spindle microtubules.

There are several mechanisms by which aberrant spindle morphology and mitotic block could result from stabilization of microtubule dynamics by taxol. For example, during prometaphase, the plus ends of dynamic spindle microtubules appear to probe the cytoplasm until linkage with a chromosomal kinetochore is established (22, 23). Reduced microtubule dynamics in the presence of taxol could result in the attachment of fewer than a normal number of microtubules to the kinetochores, as occurs with vinblastine (9), which may lead to failure of chromosome congression (Fig. 2 *d–i*). In addition, we were surprised to find, given the ability of taxol at high concentrations to enhance microtubule polymerization, that taxol, like vinblastine, nocodazole, podophyllotoxin (8), and estramustine (24), induced shortening of the microtubules of the central spindle and decreased separation of spindle poles (Table 1). Microtubules of the central spindle region flux or treadmill in a poleward direction during metaphase and anaphase (25, 26). Taxol, like vinblastine, colchicine, podophyllotoxin, and nocodazole, inhibits treadmilling or flux of microtubules *in vitro* (refs. 10 and 27–29, and L.W., unpublished data), and shorter central spindles may be due to a reduced flux rate. In addition, the

transition from metaphase to anaphase may require dynamic spindle microtubules for correct spindle formation, for chromosome separation, or for a thus far unknown signaling mechanism.

At taxol concentrations >10 nM, the mass of microtubule polymer in cells increased, attaining levels that were 500% of controls at high taxol concentrations (330 nM). Microtubule bundles became prominent in this concentration range (Fig. 3). Increased microtubule polymer mass and induction of massive bundles of microtubules may contribute to the antiproliferative action of taxol at high concentrations. However, increased polymer mass and induction of microtubule bundling did not occur at the lowest effective concentrations of taxol, so neither action of the drug can account for inhibition of proliferation by low concentrations of the drug. It is curious that even with a large excess of stabilized microtubules, the interphase microtubule cytoskeleton can depolymerize or rearrange sufficiently for the cell to enter mitosis and construct a mitotic-like spindle. In addition, it appears that either the dynamics of mitotic microtubules are more sensitive than those of interphase microtubules to stabilization by taxol or that stabilization of microtubule dynamics in interphase does not prevent cell cycle progression through interphase in HeLa cells.

At high concentrations, taxol binds stoichiometrically to tubulin in microtubules (3, 21). However, taxol suppresses dynamic instability of bovine brain microtubules *in vitro* at taxol/tubulin ratios as low as 1:150 (Table 2). Under conditions of the most sensitive mitotic block in the present work (3–10 nM taxol), the intracellular taxol concentration is 40–70% less than the concentration of tubulin in microtubule polymer (Table 1). Although the mechanism of inhibition of microtubule dynamics by taxol has not been elucidated, these results indicate that inhibition of microtubule dynamics and inhibition of mitosis may result from the binding of small numbers of taxol molecules per microtubule.

Taxol shares with vinblastine, nocodazole, colchicine, and podophylloxin the ability to block mitosis at low drug concentrations in the presence of normal amounts of microtubule polymer and with a similar aberrant spindle organization (8, 12). All five compounds inhibit treadmilling of microtubules in the absence of changes in the polymer mass (refs. 10 and 27–29 and L.W., unpublished data). In addition, taxol, vinblastine, nocodazole, and colchicine suppress microtubule dynamic instability in the absence of significant changes in the microtubule polymer mass (Table 2 and refs. 11, 12, and 30). Thus, the similar actions of these drugs on microtubules *in vivo* and *in vitro* suggest that low concentrations of taxol, like low concentrations of other antimitotic drugs, block mitosis and inhibit cell proliferation by inhibiting the dynamics of spindle microtubules.

The taxol concentrations used in the present study are considerably lower than those currently used clinically; e.g., a steady-state plasma taxol concentration of 0.45 μM was reported during a 24-h continuous intravenous infusion of 170 mg of taxol per m^2 (31). These results, as well as evidence that low concentrations of taxol enhance the cytotoxicity of estramustine (32), suggest that therapeutic administration of lower taxol concentrations than presently used might effectively inhibit tumor cell growth. In support of this idea, recent evidence indicates that mitotic block induced in HeLa cells by taxol at low concentrations leads not only to inhibition of cell proliferation but also to cell killing (M.A.J. and L.W., unpublished data).

We thank Ms. Kim Wendell, Ms. Sara Gardiner, and Mr. Herb Miller for excellent technical assistance and Mr. Brent Derry for careful reading of the manuscript and for measurements of critical concentration. This work was supported by Grant CA57291-01 from the National Cancer Institute (M.A.J.) and by Grant DHP-43E from the American Cancer Society (L.W.).

1. Rowinsky, E. K. & Donehower, R. C. (1991) *Pharmacol. Ther.* **52,** 35–84.
2. Schiff, P. B., Fant, J. & Horwitz, S. B. (1979) *Nature (London)* **277,** 665–667.
3. Parness, J. & Horwitz, S. (1981) *J. Cell Biol.* **91,** 479–487.
4. Fuchs, D. A. & Johnson, R. K. (1978) *Cancer Treat. Rep.* **62,** 1219–1222.
5. Schiff, P. B. & Horwitz, S. B. (1980) *Proc. Natl. Acad. Sci. USA* **77,** 1561–1565.
6. Rowinsky, E. K., Donehower, R. C., Jones, R. J. & Tucker, R. W. (1988) *Cancer Res.* **48,** 4093–4100.
7. Jordan, M. A., Thrower, D. & Wilson, L. (1991) *Cancer Res.* **51,** 2212–2222.
8. Jordan, M. A., Thrower, D. & Wilson, L. (1992) *J. Cell Sci.* **102,** 401–416.
9. Wendell, K. L., Wilson, L. & Jordan, M. A. (1993) *J. Cell Sci.* **104,** 261–274.
10. Jordan, M. A. & Wilson, L. (1990) *Biochemistry* **29,** 2730–2739.
11. Toso, R. J., Jordan, M. A., Farrell, K. W., Matsumoto, B. & Wilson, L. (1993) *Biochemistry* **32,** 1285–1293.
12. Wilson, L. & Jordan, M. A. (1993) in *Microtubules*, ed. Hyams, J. & Lloyd, C. (Wiley, New York), in press.
13. Thrower, D., Jordan, M. A. & Wilson, L. (1991) *J. Immunol. Methods* **136,** 45–51.
14. Levan, A. (1938) *Hereditas* **24,** 471–486.
15. Amin-Hanjani, S. & Wadsworth, P. (1991) *Cell Motil. Cytoskeleton* **20,** 136–144.
16. DeBrabander, M., Geuens, G., Nuydens, R., Willebrords, R. & De Mey, J. (1981) *Proc. Natl. Acad. Sci. USA* **78,** 5608–5612.
17. Kallajoki, M., Weber, K. & Osborn, M. (1992) *J. Cell Sci.* **102,** 91–102.
18. Manfredi, J. J., Parness, J. & Horwitz, S. B. (1982) *J. Cell Biol.* **94,** 688–696.
19. Jordan, M. A., Margolis, R. L., Himes, R. H. & Wilson, L. (1986) *J. Mol. Biol.* **187,** 61–73.
20. Singer, W. D., Jordan, M. A., Wilson, L. & Himes, R. H. (1989) *Mol. Pharmacol.* **36,** 366–370.
21. Diaz, J. F. & Andreu, J. M. (1993) *Biochemistry* **32,** 2747–2755.
22. Rieder, C. L., Alexander, S. P. & Rupp, G. (1990) *J. Cell Biol.* **110,** 81–95.
23. Hayden, J. H., Bowser, S. S. & Rieder, C. L. (1990) *J. Cell Biol.* **111,** 1039–1046.
24. Sheridan, R. V., Speicher, L. A. & Tew, K. D. (1991) *Eur. J. Cell Biol.* **54,** 268–276.
25. Mitchison, T. (1989) *J. Cell Biol.* **45,** 515–527.
26. Mitchison, T. J. & Salmon, E. D. (1992) *J. Cell Biol.* **119,** 569–582.
27. Wilson, L., Miller, H. P., Farrell, K. W., Snyder, K. B., Thompson, W. C. & Purich, D. L. (1985) *Biochemistry* **24,** 5254–5262.
28. Wilson, L. & Farrell, K. W. (1986) *Ann. N.Y. Acad. Sci.* **466,** 690–708.
29. Jordan, M. A. & Farrell, K. W. (1983) *Anal. Biochem.* **130,** 41–53.
30. Wilson, L., Toso, R. J. & Jordan, M. A. (1993) *Cell. Pharmacol.*, suppl. 1, in press.
31. Reed, E., Sarosy, G., Jamis-Dow, C., Klecher, R., Kohn, E., Link, C., Christian, M., Davis, P. & Collins, J. (1993) *Proc. Am. Assoc. Cancer Res.* **34,** 395 (abstr.).
32. Speicher, L. A., Barone, L. & Tew, K. D. (1992) *Cancer Res.* **52,** 4433–4440.